Full Length Research Article

Advancements in Life Sciences – International Quarterly Journal of Biological Sciences

Author's Affiliation:
Department of Biology, College
of Science, University of Hail -
Saudi Arabia

*Corresponding Author:
Arshad Jamal
Email:
arshadjamalus@yahoo.com

Open Access

Identification of phytochemicals as potential inhibitors against E6 protein of High-Risk Human Papillomavirus 16(HPV 16) via In-Silico Structure-Based Virtual Screening Approach

Arshad Jamal

Abstract

Background: The human papillomavirus (HPV) is a potentially fatal infection and the most common cause of cancer related feminine mortality around the world, thus requiring the design of anticancer drugs. The E6 oncoprotein is one of the most investigated therapeutic targets for cancer treatment. E6 oncoprotein plays a major role in tumor progression and cell immortalization. The E6 protein leads to the degradation of tumor suppressor protein P53 via interacting with E6 binding protein E6AP. Therefore, inhibiting the E6 protein can be a potential target for HPV.

Methods: In this study we performed virtual screening of 2296 phytochemicals library from MPD3 database against E6 protein.

Results: Three compounds were picked out as potential inhibitors. These compounds were selected considering their binding energy and hydrogen bond interactions. Further to verify the stability of the docked complexes 100ns molecular dynamics simulations were carried out.

Conclusion: Keeping in view the numerous analyses, we suggest that the potential three compounds could prove relevancy regarding the anti-HPV therapeutic advancements.

Introduction

Human Papillomavirus (HPV) is a highly contagious and commonly sexually transmitted human pathogen. HPVs are DNA viruses that infect and reproduce in keratinized and mucosal epithelia, resulting in unusual hyperplastic lesions[1]. HPV consists of two kinds of genes, which includes early gene (E) and late genes (L) [2] having different roles such as regulation of the replication process, virus assembly and development of a tumor or cancerous Lesions [3]. Most of HPV genotypes which predominantly cause benign skin warts and anogenital lesions are considered as low-risk. Laryngo bronchial systems and papillomatosis are also caused by harmless HPV genotypes. Whilst the most dangerous HPV genotypes like HPV_16 and HPV-18 are predominantly responsible for causing cervical cancer and urogenital malignancies [4]. HPV is responsible for more than 5% of all malignancies in the world, such as all cervical cancers and oropharyngeal cancers [5, 6]. Regardless of considerably lower cervical cancer incidence in developed countries with established screening programs, cervical cancer is considered one of the highest reasons of cancer mediated mortality in female globally, owing to a lack of resources. HPV-related oropharyngeal cancer is just one of five malignancies in the United States that has increased in incidence since 1975 and has now surpassed the cervix as the most prevalent site of HPV-related cancer [7]. Genome of HPV encodes six early proteins E1, E2, E4, E5, E6 and E7 as well as two late proteins such as L1 and L2. However, E6 and E7 viral proteins have been identified as essential participants in the production and maintenance of HPV-related cervical cancer [5]. HPV oncoproteins such as E6 act by binding to p53 protein, as a result triggering degradation via proteasomes [8].

The HPV E6 protein is one of three oncoproteins encoded by the virus. It has been implicated a powerful oncogene and has also suggested for its role in the events leading to the malignant transformation of virally infected cells [9]. The E6 proteins are not long polypeptides, consisting of around 150 amino acids and have two Zinc- Finger domains E6C and E6N [10-13]. The E6C domain of HPV16 remains monomeric, while the E6N domain homodimerizes at high concentrations. Since E6 oncoproteins trigger p53 degradation, which is associated with tumor progression. Hence E6 has been suggested as the best possible cancer therapeutic agent [14]. The HPV viral infection degrades the activation of tumor suppressor protein p53 [15]. HPV oncoproteins such as E6 act by binding to p53 protein, as a result triggering degradation via proteasomes [8].

The intracellular accretion of the two oncoproteins, E6 and E7, is a significant molecular determinant of HPV-induced keratinocyte transformation [16]. Notably, the E6 plays a vital part in cancer growth and progression because of its significant inhibition effects on numerous onco suppressor signalling pathways such as P53 pathway. E6 not have enzymatic activity and relies primarily on protein-protein interactions (PPIs) to carry out its tasks [17].

The well-studied function of E6 protein is to target the degradation of P53 protein through the recruitment of E6AP [18]. Interestingly, HPV-transformed cells survival depends on the persistent expression of E6, as the inhibition leads to reactivation of p53-arbitrated pathways resulting in a p53-dependent senescence and apoptosis in HPV-positive cancer cells [19]. The P53 suppressor protein is functionally changed or mutated in most cancers, such as in epithelial tumors, including human cervical cancer and head and neck cancer [20] [10]. Therefore, E6 is a preferred target for HPV treatment [21]. Numerous studies have been done to test the E6-E6Ap interaction inhibition by different molecules such as intrabodies [22], alpha helical peptides [23] and small molecules [24] [25]. Lee et al. extracted Jaceosidin using methanol extract of *Artemisia argyi* and found that it inhibited the binding of oncoprotein to the P53 protein [9]. However, the majority of the molecules showed only moderate action or has a low bioavailability. Hence, there is still a need to identify pharmacologically active compounds for the treatment of HPV. Drug development, on the other hand, is a time- and money-intensive process that takes more than a decade and costs an average of $2.8 billion per approved drug [26]. Computer-aided drug discovery (CADD) is a striking addition to drug development, especially in the early stages. CADD aims to increase the efficacy of hit discovery by testing and screening large compound libraries in-silico in order to discover a limited number of candidates with desired pharmacological features. The CADD improved the drug discovery process by making it more goal-oriented, saving time and money [27]. In this study we performed in-silico screening of a library of phytochemicals to select potential inhibitors for HPV oncoprotein E6. To confirm the stability of the ligand-protein complexes molecular dynamics simulations and free binding energy analysis were performed.

Methods

Ligand Database Preparation

A data set of 2096 phytochemicals was downloaded from the MPD3 database[28]. Employing Autodock tools optimization was carried out for all the compounds prior to docking. Gassteiger charges were optimized of all the compounds. Only polar hydrogens were added to the compounds. After that these

optimized compounds were saved in pdbqt format for docking experiments.

Preparation of Receptor and virtual screening

The 3D crystallographic structure of the HPV-E6 protein bound P53 and E6AP was downloaded using the PDB database (PDB ID 4XR8). P53 protein and E6AP and other crystallographic molecules were removed from the E6 protein. The E6 protein structure was prepared for docking purpose utilizing the Autodock Tools. Gassteiger charges and polar hydrogens were introduced to the protein structure. Later on, the structure was saved in pdbqt format for eventual docking purpose. The size of the Grid box was set to 60 Å x 60 Å x 60 Å and the centered around the residues of the E6 protein which involves in binding to the P53. Total 20 poses were generated for each compound and docked poses were analyzed based on the binding energy scores.

Molecular Dynamics Simulations

To better understand the stability of the ligand-protein complexes Molecular Dynamics simulations were performed on the final selected inhibitors and Apo structure of the HPV-E6 protein using GROMACS [29]. CHARMM36 force field was utilized to prepare the topology of the receptor protein and to prepare the topology of ligand, CHARMM General Force Field (CGenFF) was used [30, 31]. All the complexes were solved in the octahedral box and TIP3 water model. Negative ions (CL) were added to the systems to neutralize the systems. A number of 10000 steps of steepest descent method was performed to minimize all the systems. The temperature of the systems was equilibrated from 0 to 300k gradually using NVT ensemble. Furthermore, the systems were simulated under NPT ensemble at a pressure of 1.0 bar and temperature 300 K. Particle Mesh Ewald method was used for long range electrostatic and a distance cut off was set to 10 Å for short range electrostatic and Vander Waals [32]. Linear Constraints Solver (LINCS) algorithm was applied to constrain all bonds [33]. Finally production run of 100ns was performed for all complexes and trajectories were saved after each 2fs.

MM/PBSA Binding Free Energy Calculation

The MM/PBSA method is widely utilized to calculate the binding free energies of protein-ligand complexes. [34, 36]. G_mmpbsa module of GROMACS was used to calculate the binding energy of the simulated complexes [37]. To calculate the binding free energy snapshots from the last 30ns of the trajectory were extracted.

Results

Docking of Jaceosidin with E6

In order to have better understanding of the interaction between E6 and P53, we initiated the analysis by studying the interface of E6 and P53 complex (Figure 1A). These residue Arg10, Ala46, Phe47, Asp49, Cys51,Ser97, Asp98, Leu99, Leu100, Ile101, Proline109, Arg131 and CQKPLCPEEK(106-115) of E6 protein make interactions with the P53 contributing the stability of complex (Figure 1B) [38]. We also docked Jaceosidin inhibitor to E6 protein to observe the interactions between Jaceosidin and E6. Jaceosidin has been reported as potent inhibitor against oncoproteins and tumor suppressor p53. The binding energy score of the Jaceosidin-E6 complex was -7.1 kcal. Jaceosidin formed hydrogen bonds with Tyr32, Tyr70, Ser71, Gln07, Arg131, and Arg129 (Figure 2A).
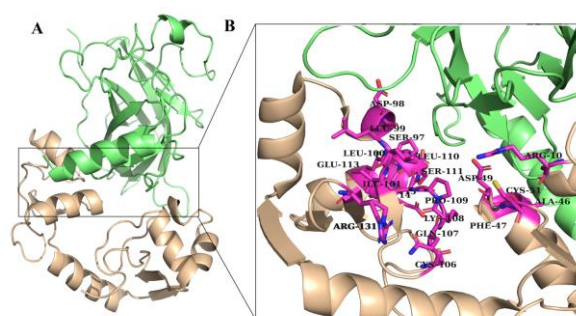

Figure 1: A) E6 and P53 protein complex B) The interface residues od E6 shown in pink sticks interacting with the P53 (green).

Molecular Docking

The current study demonstrated a virtual screening of phytochemicals library antagonizing E6 protein using Autodock Vina. After virtual screening the compounds were categorized considering their binding scores (kcal/mol). In total 2296 natural compounds were docked to the P53 binding site of E6. After docking the top 150 compounds were visually analyzed. Compounds making hydrogen bond interactions with the important interface residues of E6 were selected. Three compounds PubChem ID 11685925, ZINC ID 150605978 and ZINC ID42803913 were selected for further analysis on the bases of energy score and hydrogen bond interactions. These three compounds were taken as promising candidates for subsequent studies. The chemical properties of the top selected compounds are shown in Table 1. The final selected compounds PubChem ID 11685925, ZINC ID150605978 and ZINC ID42803913 have energy -9.8 Kcal/mol, -9.8Kcal/mol and -10.4 Kcal/mol. Out of these three compounds ZINC ID 150605978 formed highest number of Hydrogen bonds with binding energy -9.8Kcal. This compound made hydrogen bonds with 8 residues Tyr70, Ser71, Ser74, Arg77, Arg102, Gln107, Arg129, Trp132 were observed. Out of 8 residues the four hydrogen bonds (Tyr70, Tyr71, Gln107 and Arg 129)

were also observed in Jaceosidin. Compound PubChem ID 11685925 and ZINC ID42803913 formed four hydrogen bonds. Compound PubChem ID 11685925 made hydrogen bonds with Tyr70, Ser74, ARg131 and Arg129 .Three hydrogen bonds (Tyre70, Arg131 and Arg129) were also observed in Jaceosidin. Compound ZINC ID42803913 made hydrogen bonds with Tyr32, Ser71, Gln107 and Arg131 showing strong binding affinity. All these four hydrogen bonds were also observed in Jaceosidin. The binding energy of all the compounds is less than Jaceosidin. The lower binding energy of the top picked candidates compared to the well-known inhibitor in the respective docking complexes suggests that the novel leads exhibit robust binding into the active site of E6 than its established inhibitor Jaceosidin.
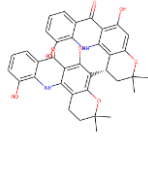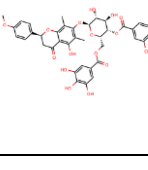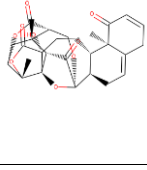
Compound ID	Chemical Structure	Molecular Formula	Molecular Weight	Logp
PubChem ID 11685925		$C_{36}H_{32}N_2O_8$	620.6	7.1
ZINCID 150605978		C38H36O18	780.688	2.866
ZINC ID42803913		C28H30O9	510.539	1.55

Table 1: Properties of the final selected compounds.

Compound ID	Binding Energy Score (Kcal/mol)	Residues making H-bonds	No. of H-bonds
Jaceosidin	-7.1	Tyr32, Tyr70, Ser71,Gln107, Arg131, Arg129	7
PubChem ID 11685925	-9.8	Tyr70, Ser74, ARg131, Arg129	4
ZINC ID 150605978	-9.8	Tyr70,Ser71,Ser74,Arg77,Arg102, Gln107,Arg129,Trp132	14
ZINC ID 42803913	-10.4	Tyr32, Ser71, Gln107, Arg131	5

Table 2: Binding energy values of the top selected compounds and the residues making hydrogen bonds with the compounds.

Molecular Dynamics Simulations

To recognize the stability of the complexes, molecular dynamics simulations were performed. To identify the system equilibrium, the root-mean-square deviation (RMSD) values of the backbone atoms were compared to the corresponding beginning structures in all simulations. It is a known fact that the smaller RMSD

values of one simulation indicate a stable state of the system however; the larger RMSD values point out large conformational changes of the investigated system [39]. Figure 3A shows RMSD of Apo-E6 and three complexes plotted over the time of 100ns. A close analysis of the RMSD plot for all the systems clearly suggests that all the complexes were stable as compared to the Apo-E6. Compound PubChem ID 11685925 and compound ZINC ID 150605978 remained more stable through the whole simulation time with average RMSD 0.30 and 0.31 nm, while compound ZINC ID 42803913 was stable till 70ns but fluctuated a little bit after that till the end of the simulation.
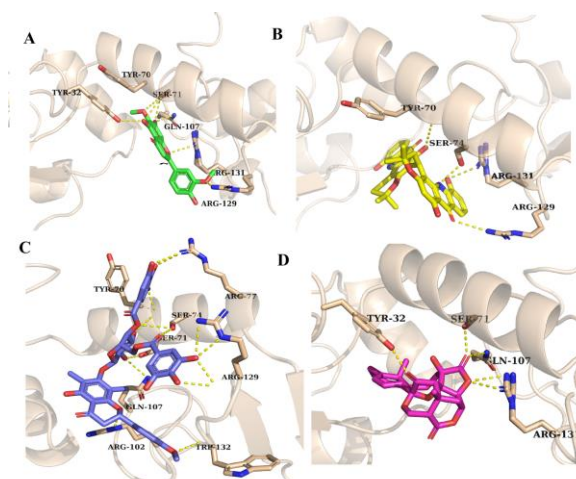

Figure 2: Docked conformations of the final selected compounds, Residues making hydrogen bonds are shown in sticks. A) Jaceosidin B) PubChem ID 11685925 C) ZINC ID 150605978 D) ZINC ID 42803913

To examine the conformational variability of each trajectory, root mean square fluctuations (RMSF) of protein residues was plotted against the residue number to show the local conformational changes for all the four simulations (Figure 3B). The average RMSF of all the three complexes is roughly the same. The average RMSF of overall positions are 0.21nm for PubChem ID 11685925, 0.20nm for ZINC ID 150605978 and 0.24nm for ZINC ID 42803913. The Apo-E6 exhibited prominent conformational changes throughout the 100ns simulation time indicating that the complexes remained stable as compared to the Apo state.

Radius of gyration (Rg), Solvent accessible surface area (SASA) and Hydrogen bonds

The Rg suggests the density of the system, and eventually controlling the folding rate and stability of proteins. Rg was determined to test the compactness of all the complexes. Furthermore, we found out that Rg of all complexes was persistent with the RMSD of system. Figure 4A indicates that all the ligand-protein

complex system remained compact as compared to the Apo-E6. In Apo state the E6 proteins structure as illustrated by higher Rg.
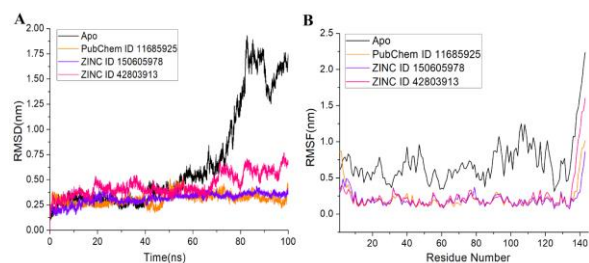

Figure 3: A) Demonstrate RMSD of Apo-E6 and three complexes plotted over the time of 100ns. A close analysis of the RMSD plot for all the systems clearly suggests that all the complexes were stable as compared to the Apo-E6. **B)** root mean square fluctuations (RMSF) of protein residues was plotted with respect to the residue number to show the local conformational changes for all the four simulations.

SASA is yet another tool that plays a critical role in the maintenance of protein stability, folding, and conformational changes. SASA was estimated using gmx sasa module for a simulation period of 100 ns (Figure 4B). Average SASA values for all the systems were monitored. The average SASA values of the Apo-E6, PubChem ID 11685925, ZINC ID 150605978 and ZINC ID 42803913were found to be 103.71 nm^2, 98.45 nm^2, and 99.75 nm^2, and 101.03nm^2 respectively. The accessible surface area of all the complexes under investigation didn't alter throughout the simulation time indicating that there were no major changes in the accessible surface area of the protein, while the accessibility area of the Apo-E6 system exposed more after 60ns simulation time. The change in the exposed surface area of the Apo state could be due to the more exposed conformation to solvent.

Hydrogen bonding, in ligand-protein complexes, is a key factor for the stability of the complexes. High number of hydrogen bonds were observed between ZINC ID 150605978 and ZINC ID 42803913 compared to PubChem ID 11685925. The hydrogen–bond interaction pattern of ZINC ID 50605978 and ZINC ID 42803913 remained quite stable throughout the simulation, indicating that these ligand–protein complexes are stable in particular (Figure 4C).

MM/PBSA Binding Free Energy Calculation

To elaborate the binding energy of the compounds NPACT01552 with the E6 protein quantitatively, we performed the MM/PBSA calculations. The binding free energies and energy components are mentioned in Table 3. The calculated bind free energy of complex PubChem ID 11685925 is -160.413±17.509 kJ/mol, ZINC ID 50605978 is -120.711±15.567kJ/mol and of complex ZINC ID 42803913 is -80.063±14.429 kJ/mol. The van

der Waals energy term (ΔEvdw) and SAS (ΔESA) were the major contributors to the binding free energy in complexes PubChem ID 1685925 and ZINC ID 50605978,while in case of ZINC ID 42803913 the ΔEvdw and ΔE$_{elec}$ contributed significantly to the binding energy.
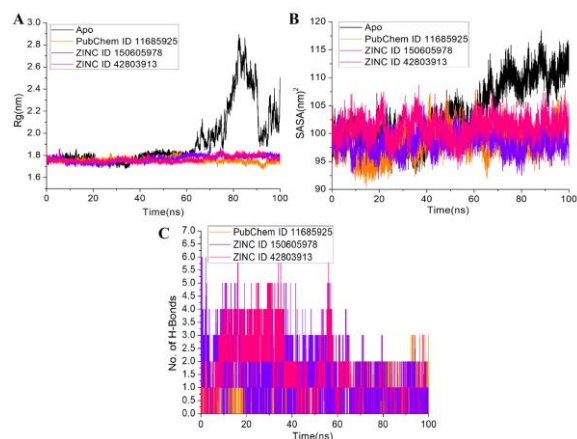

Figure 4: A) Indicate that all the ligand-protein complex system remained compact as compared to the Apo-E6. In Apo state the E6 proteins structure as illustrated by higher Rg. **B)** SASA was estimated using gmx sasa module for a simulation period of 100 ns. **C)** High number of hydrogen bonds were observed between ZINC ID 150605978 and ZINC ID 42803913 compared to PubChem ID 11685925.

Energy Terms	PubChem ID 11685925	ZINC ID 150605978	Energy Terms
ΔE$_{vdw}$ (KJ/mol)	-180.089± 13.662	-207.563±12.227	-119.906±13.852
ΔE$_{elec}$ (KJ/mol)	-15.897 ±9.147	-4.889± 9.997	-32.406±7.242
ΔESA (KJ/mol)	-20.098±1.398	-22.341±1.294	-16.192±2.046
ΔE$_{polar}$ (KJ/mol)	55.670 ±15.967	114.082± 14.998	88.441±16.691
ΔE$_{binding}$ (KJ/mol)	-160.413±17.509	-120.711±15.567	-80.063±14.429

Table 3: Binding Free energy (kJ/mol) analysis of the simulated systems. ΔEvdw: van der Waals interaction energy; ΔEelec: electrostatic interaction energy; ΔESA: SAS energy; ΔEpolar: polar solvation energy; ΔEbinding: binding energy.

Discussion

In the current study we performed in-silico screening of a library of phytochemicals to select potential inhibitors for HPV oncoprotein E6. The HPV E6 protein is one of three oncoproteins encoded by the virus. It has been implicated a powerful oncogene and has also suggested for its role in the events leading to the malignant transformation of virally infected cells [9]. The well-studied function of E6 protein is to target the degradation of P53 protein through the recruitment of E6AP [18]. To confirm the stability of the ligand-protein complexes molecular dynamics simulations and free binding energy analysis were performed.

To have better understanding of the interaction between E6 and P53, we initiated the analysis by

studying the interface of E6 and P53 complex (Figure 1A). These residue Arg10, Ala46, Phe47, Asp49, Cys51,Ser97, Asp98, Leu99, Leu100, Ile101, Proline109, Arg131 and CQKPLCPEEK(106-115) of E6 protein make interactions with the P53 contributing the stability of complex (Figure 1B) [38]. Furthermore, we performed the docking of Jaceosidin inhibitor to E6 protein to observe the interactions between Jaceosidin and E6 [19]. Jaceosidin is a known inhibitor of oncoproteins and tumor suppressor p53 [22].

The current study demonstrated a virtual screening of phytochemicals library antagonizing E6 protein using Autodock Vina. After virtual screening the compounds were categorized considering their binding scores (kcal/mol). In total 2296 natural compounds were docked to the P53 binding site of E6. After docking the top 150 compounds were visually analyzed. Compounds making hydrogen bond interactions with the important interface residues of E6 were selected. Three compounds PubChem ID 11685925, ZINCID 150605978 and ZINC ID42803913 (-9.8 Kcal/mol, -9.8Kcal/mol and -10.4 Kcal/mol respectively) were selected for further analysis on the bases of energy score and hydrogen bond interactions. The chemical properties of the top selected compounds are shown in Table 1. This ZINCID 150605978 made hydrogen bonds with 8 residues Tyr70, Ser71, Ser74, Arg77, Arg102, Gln107, Arg129, Trp132 were observed. Out of 8 residues the four hydrogen bonds (Tyr70, Tyr71, Gln107 and Arg 129) were also observed in Jaceosidin (11). Compound PubChem ID 11685925 and ZINC ID42803913 formed four hydrogen bonds. Compound PubChem ID 11685925 made hydrogen bonds with Tyr70, Ser74, ARg131 and Arg129. Three hydrogen bonds (Tyre70, Arg131 and Arg129) were also observed in Jaceosidin [8]. Compound ZINC ID42803913 made hydrogen bonds with Tyr32, Ser71, Gln107 and Arg131 showing strong binding affinity. All these four hydrogen bonds were also observed in Jaceosidin [23].

The binding energy of all the compounds is less than Jaceosidin. The lower binding energy of the top picked candidates compared to the well-known inhibitor in the respective docking complexes suggests that the novel leads exhibit robust binding into the active site of E6 than its established inhibitor Jaceosidin [35].

To determine the stability of the complexes, molecular dynamics simulations were performed. To identify the system equilibrium, the RMSD values of the backbone atoms were compared to the corresponding beginning structures in all simulations. It is a known fact that the smaller RMSD values of one simulation indicate a stable state of the system however; the larger RMSD values point out large conformational changes of the investigated system [39]. Figure 3A shows RMSD of Apo-E6 and three

complexes plotted over the time of 100ns are constantly stable. To investigate the conformational variability of each trajectory, RMSF of protein residues was plotted against the residue number to show the local conformational changes for all the four simulations. The Apo-E6 exhibite prominent conformational changes throughout the 100ns simulation time indicating that the complexes remained stable as compared to the Apo state.

Moreover, our Rg (compactness of the complexes) and SASA (maintenance of protein stability, folding, and conformational changes) calculations and estimations were persistent with the RMSD [7, 32]. Thereby indicating stable density of the system, the folding rate and stability of proteins. Furthermore, the binding stability of the compounds was confirmed by the binding free energy method. Apparently, these findings were consistent with the docking and simulation results suggesting that these compounds may act as potential inhibitors of HPV-16 E6 protein.

In this study we used an integrated strategy of virtual screening and molecular dynamics simulations to find potent inhibitors from the phytochemical's library antagonizing HPV-16 E6 protein. Potent HPV-16 E6 protein inactivates p53 by triggering its degradation. Therefore, the E6 protein is of substantial relevance for the development of new inhibitors to combat the problems of cervical cancer. Presumably, plant-derived phytochemicals and derivatives exhibit therapeutic potency offering minimal side effects in cancer patients. Many of these phytochemicals are naturally occurring bioactive compounds with high antitumor potential. Three compounds (PubChem ID 11685925, ZINC ID 150605978 and ZINC ID 42803913) were shortlisted as lead inhibitors against E6 protein. These molecules exhibited good binding affinity and stable binding modes as predicted by molecular docking and molecular dynamics simulations. Furthermore, the binding stability of the compounds was confirmed by the binding free energy method. Apparently, these findings were consistent with the docking and simulation results suggesting that these compounds may act as potential inhibitors of HPV-16 E6 protein.

Competing Interest

The authors declare that there is no conflict of interest.

References

1. Egawa N, Egawa K, Griffin H, Doorbar J. Human papillomaviruses; epithelial tropisms, and the development of neoplasia. Viruses, (2015); 7(7): 3863-3890.
2. Mirabello L, Yeager M, Cullen M, Boland JF, Chen Z, et al. HPV16 sublineage associations with histology-specific cancer risk using HPV whole-genome sequences in 3200 women. JNCI: Journal of the National Cancer Institute, (2016); 108(9): djw100.

3. Bansal A, Singh MP, Rai B. Human papillomavirus-associated cancers: A growing global problem. International Journal of Applied and Basic Medical Research, (2016); 6(2): 84.

4. Palma S, Gnambs T, Crevenna R, Jordakieva G. Airborne human papillomavirus (HPV) transmission risk during ablation procedures: A systematic review and meta-analysis. Environmental Research, (2021); 192110437.

5. De Martel C, Ferlay J, Franceschi S, Vignat J, Bray F, et al. Global burden of cancers attributable to infections in 2008: a review and synthetic analysis. The lancet oncology, (2012); 13(6): 607-615.

6. De Martel C, Plummer M, Vignat J, Franceschi S. Worldwide burden of cancer attributable to HPV by site, country and HPV type. International journal of cancer, (2017); 141(4): 664-670.

7. Berman TA, Schiller JT. Human papillomavirus in cervical cancer and oropharyngeal cancer: one cause, two diseases. Cancer, (2017); 123(12): 2219-2229.

8. Tomaić V. Functional roles of E6 and E7 oncoproteins in HPV-induced malignancies at diverse anatomical sites. Cancers, (2016); 8(10): 95.

9. Mantovani F, Banks L. The human papillomavirus E6 protein and its contribution to malignant progression. Oncogene, (2001); 20(54): 7874-7887.

10. Scheffner M, Werness BA, Huibregtse JM, Levine AJ, Howley PM. The E6 oncoprotein encoded by human papillomavirus types 16 and 18 promotes the degradation of p53. cell, (1990); 63(6): 1129-1136.

11. Lipari F, McGibbon GA, Wardrop E, Cordingley MG. Purification and biophysical characterization of a minimal functional domain and of an N-terminal Zn2+-binding fragment from the human papillomavirus type 16 E6 protein. Biochemistry, (2001); 40(5): 1196-1204.

12. Grossman S, Laimins L. E6 protein of human papillomavirus type 18 binds zinc. Oncogene, (1989); 4(9): 1089-1093.

13. Barbosa MS, Lowy DR, Schiller JT. Papillomavirus polypeptides E6 and E7 are zinc-binding proteins. Journal of virology, (1989); 63(3): 1404-1407.

14. Celegato M, Messa L, Goracci L, Mercorelli B, Bertagnin C, et al. A novel small-molecule inhibitor of the human papillomavirus E6-p53 interaction that reactivates p53 function and blocks cancer cells growth. Cancer Letters, (2020); 470115-125.

15. Travé G, Zanier K. HPV-mediated inactivation of tumor suppressor p53. Cell Cycle, (2016); 15(17): 2231-2232.

16. Tommasino M. The human papillomavirus family and its role in carcinogenesis; 2014. Elsevier. pp. 13-21.

17. Howie HL, Katzenellenbogen RA, Galloway DA. Papillomavirus E6 proteins. Virology, (2009); 384(2): 324-334.

18. Martinez-Zapien D, Ruiz FX, Poirson J, Mitschler A, Ramirez J, et al. Structure of the E6/E6AP/p53 complex required for HPV-mediated degradation of p53. Nature, (2016); 529(7587): 541-545.

19. Li C, Johnson DE. Liberation of functional p53 by proteasome inhibition in human papilloma virus-positive head and neck squamous cell carcinoma cells promotes apoptosis and cell cycle arrest. Cell cycle, (2013); 12(6): 923-934.

20. Bosch FX, Broker TR, Forman D, Moscicki A-B, Gillison ML, et al. Comprehensive control of human papillomavirus infections and related diseases. Vaccine, (2013); 31H1-H31.

21. Manzo-Merino J, Thomas M, Fuentes-Gonzalez AM, Lizano M, Banks L. HPV E6 oncoprotein as a potential therapeutic target in HPV related cancers. Expert opinion on therapeutic targets, (2013); 17(11): 1357-1368.

22. Griffin H, Elston R, Jackson D, Ansell K, Coleman M, et al. Inhibition of papillomavirus protein function in cervical cancer cells by intrabody targeting. Journal of molecular biology, (2006); 355(3): 360-378.

23. Liu Y, Liu Z, Androphy E, Chen J, Baleja JD. Design and characterization of helical peptides that inhibit the E6 protein of papillomavirus. Biochemistry, (2004); 43(23): 7421-7431.

24. Baleja JD, Cherry JJ, Liu Z, Gao H, Nicklaus MC, et al. Identification of inhibitors to papillomavirus type 16 E6 protein based on three-dimensional structures of interacting proteins. Antiviral research, (2006); 72(1): 49-59.

25. Malecka KA, Fera D, Schultz DC, Hodawadekar S, Reichman M, et al. Identification and characterization of small molecule human papillomavirus E6 inhibitors. ACS chemical biology, (2014); 9(7): 1603-1612.

26. DiMasi JA, Grabowski HG, Hansen RW. Innovation in the pharmaceutical industry: new estimates of R&D costs. Journal of health economics, (2016); 4720-33.

27. Vickers NJ. Animal communication: when i'm calling you, will you answer too? Current biology, (2017); 27(14): R713-R715.

28. Mumtaz A, Ashfaq UA, ul Qamar MT, Anwar F, Gulzar F, et al. MPD3: a useful medicinal plants database for drug designing. Natural product research, (2017); 31(11): 1228-1236.

29. Van Der Spoel D, Lindahl E, Hess B, Groenhof G, Mark AE, et al. GROMACS: fast, flexible, and free. Journal of computational chemistry, (2005); 26(16): 1701-1718.

30. Brooks BR, Brooks III CL, Mackerell Jr AD, Nilsson L, Petrella RJ, et al. CHARMM: the biomolecular simulation program. Journal of computational chemistry, (2009); 30(10): 1545-1614.

31. Vanommeslaeghe K, Ghosh J, Polani NK, Sheetz M, Pamidighantam SV, et al. Automation of the CHARMM general force field for drug-like molecules. Biophysical Journal, (2011); 100(3): 611a.

32. Darden T. York D Pedersen L 1993 J. Chem Phys, 9810089.

33. Hess B, Bekker H, Berendsen H, Fraaije J (1997) AIDJCC4. 3.0. CO.

34. Yang T, Wu JC, Yan C, Wang Y, Luo R, et al. Virtual screening using molecular simulations. Proteins: Structure, Function, and Bioinformatics, (2011); 79(6): 1940-1951.

35. Kollman PA, Massova I, Reyes C, Kuhn B, Huo S, et al. Calculating structures and free energies of complex molecules: combining molecular mechanics and continuum models. Accounts of chemical research, (2000); 33(12): 889-897.

36. Hou T, Wang J, Li Y, Wang W. Assessing the performance of the MM/PBSA and MM/GBSA methods. 1. The accuracy of binding free energy calculations based on molecular dynamics simulations. Journal of chemical information and modeling, (2011); 51(1): 69-82.

37. Kumari R, Kumar R, Consortium OSDD, Lynn A. g_mmpbsa⊠ A GROMACS tool for high-throughput MM-PBSA calculations. Journal of chemical information and modeling, (2014); 54(7): 1951-1962.

38. Crook T, Vousden KH, Tidy JA. Degradation of p53 can be targeted by HPV E6 sequences distinct from those required for p53 binding and trans-activation. Cell, (1991); 67(3): 547-556.

39. Rungrotmongkol T, Nunthaboot N, Malaisree M, Kaiyawet N, Yotmanee P, et al. Molecular insight into the specific binding of ADP-ribose to the nsP3 macro domains of chikungunya and Venezuelan equine encephalitis viruses: molecular dynamics simulations and free energy calculations. Journal of Molecular Graphics and Modelling, (2010); 29(3): 347-353.